33rd Annual International Conference of the IEEE EMBS
Boston, Massachusetts USA, August 30 - September 3, 2011

Motor adaptation during redundant tasks with the wrist

Domenico Formica, Domenico Campolo, Fabrizio Taffoni, Flavio Keller, Eugenio Guglielmelli

Abstract— **This study analyzes motor adaptation during a redundant tasks with the wrist. The goal is threefold: (i) understanding if motor adaptation also occurs when CNS is involved in the solution of the redundancy problem; (ii) addressing whether motor strategies used to solve redundancy (i.e Donders' law) are disrupted or not during adaptation; (iii) verifying if motor strategies remain the same during adaptation and washout or they themselves adapt. First of all, our data confirm that CNS adapts its movements to the perturbation also when it is committed in the execution of a redundant task. Secondly, we showed that motor strategies used to solve redundancy (i.e Donders' law) are not disrupted during adaptation, since absolute values of thickness during the whole protocol remain in the range of physiological values. Lastly, analysis of the curvature of Donders' surfaces suggests that motor strategies, such as Donders' law, remain invariant during motor adaptation in redundant tasks.**

I. INTRODUCTION

The human motor system often needs to cope with kinematic redundancies to fulfill the requirements of everyday tasks. The brain is known to impose neural constraints to solve redundancy and optimize motor efficiency [1]-[6]. At the same time, CNS has been shown to quickly adapt motor behaviors to the changing dynamics of the body and environment [7]-[9].

Several studies tried to investigate how the CNS copes with kinematic redundancies and what are the physiological mechanisms for motor adaptation. Nevertheless, few attempts have been made to tackle both problems at the same time. Are motor adaptation and redundancy solution competing mechanisms? If yes, which has higher priority? If they are not, are they independent mechanisms, or kinematic redundancies can be exploited by the CNS to adapt faster to external perturbations [9]?

This paper aims at studying motor adaptation during a simple redundant tasks, analyzing wrist and forearm movements (3 dof system) during pointing tasks (2 dof task), and their adaptation to visual perturbation (visuomotor rotation). In previous studies we showed that, similarly to eyes movements where Donders' law applies [10], CNS solves the redundancy of such kind of tasks by imposing a motor strategy which constraints movements on 2-dimensional surfaces (called "Donders' surfaces") in the 3-D space of wrist and forearm configuration [6].

Giving to subjects a distortion of visual feedback, this study tries to investigate whether motor adaptation interferes with the natural motor strategies strategies: In particular, we want to address the following questions:

- Does motor behavior adapt to visual perturbation when CNS is also involved in the execution of a redundant task?
- If motor adaptation occurs, are motor strategies used to solve redundancy (i.e Donders' law) disrupted during adaptation?
- If they are not and Donders' law applies also during adaptation, do Donders' surfaces remain the same during the adaptation and washout phases of the protocol or they themselves adapt?

Here, we propose an experimental setup and protocol to address these issues. In particular we will assess motor learning during adaptation, analyzing the kinematics indices proposed by [11] and the motor strategies studied in [6],[12]-[13].

II. MATERIALS AND METHODS

A. Subjects

Nine right-handed healthy subjects (5 male and 4 female, aged between 24 and 28 years old), with no history of neuromuscular disorders nor previous wrist injuries, were asked to complete a series of pointing tasks with their right wrist. Right handedness for all subjects was verified by means of a standard test of laterality (Oldfield test), which has been administered to the subjects before starting the experiments.

B. Experimental setup

Each subject was strapped to a chair and to an arm-support by appropriate belts to minimize torso, shoulder and elbow movements, so that only wrist and PS forearm rotations were left unconstrained. The orientation matrix R of the wrist was measured by means of an Inertial Magnetic Unit (IMU, MTx-28A33G25 device from XSens Inc.; static orientation accuracy: < 1 deg; bandwidth: 40 Hz) mounted on top of a hollow cylindrical handle (hereafter called *hand-held* device) which each subject was asked to grasp firmly during the experiment.

The IMU, connected to a PC, was configured to continuously acquire the sequence of orientation matrices R_i (relative to the i-th sample) at a rate of 100 samples/sec. Before starting the trial, a *'zero' position* for the wrist was set

D. Formica, F. Taffoni and E. Guglielmelli are with the Laboratory of Biomedical Robotics and Biomicrosystems, Università Campus Bio-Medico di Roma, 00218 Rome, Italy. {d.formica, f.taffoni, e.guglielmelli}@unicampus.it

D. Campolo is with the School of Mechanical & Aerospace Engineering, Nanyang Technological University, 639798 Singapore, Singapore. d.campolo@ntu.edu.sg

F. Keller is with the Laboratory of Developmental Neuroscience, Università Campus Bio-Medico di Roma, 00218 Rome, Italy. f.keller@unicampus.it

to be the anatomical neutral position of the wrist, as defined by the International Standard of Biomechanics (ISB). For a generic orientation R_i, the *pointing vector*, (always parallel with the moving x-axis after the reset procedure) can then be determined as the first column of R_i:

$$\mathbf{n}_i = R_i \, [1 \; 0 \; 0]^T \tag{1}$$

A computer screen was used to display the 'video-game' according to the protocol below where (see Fig. 1) the position of a round cursor is determined, in real-time, directly by the orientation of the subject's wrist (the cursor is the projection of the pointing vector $\mathbf{n}_i$ onto the screen plane). A more detailed description of the experimental setup can be found in [6].

C. Protocol

When a session starts, the subject is instructed to move the cursor on the screen towards eight peripheral positions, in random sequence, from '1', '2', ... '8' (see in Fig. 1-left) and then back to the central position. Since the natural range of motion of the wrist is not symmetrical (the ROM of FE dof is more than double with respect to the RUD), the peripheral target positions are disposed on an ellipse, to allow subjects to span the whole natural range of motion without getting close to ROM limits. The video-game is interactive in the sense that once a highlighted target is reached by the cursor, the next target to be reached (according to the pre-computed random sequence) will be highlighted. One trial is completed after all the eight peripheral positions are reached. For each

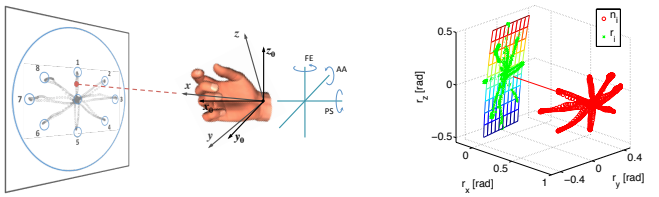

Fig. 1. Left: Typical 'video-game' for guiding a subject through pointing tasks: the subject is instructed to move the round cursor from the central position towards a peripheral position ('1', '2' ... '8'), randomly chosen by the software, and then back to the central position. Right: Rotation vectors (green crosses) are represented (in radians) in the 3-dimensional space of the motor task together with the pointing vectors (red circles). A 2-dimensional quadratic surface (Donders' surface) fits the rotation vectors.

subject, the whole experimental session is composed of 4 groups of trials:

- the first group of 5 trials, referred to as 'learning trials', are used to make the subjects acquainted with the experimental setup and with the motor task to perform. The data obtained from these trials have not been included in the analysis of results;
- the second group is composed of 5 trials, whose data are used to define the baseline of subjects' motor characteristics; these trials are named 'baseline trials';
- the third group is composed by 15 trials, where a CCW 30 deg visual rotation is fed-back to the subject. These trials are named 'adaptation trials';
- the forth group is composed by 15 trials, where the visual rotation is removed and the visual feedback is correctly displayed as in the first 10 trials of the protocol. These trials are named 'washout trials'.

For a whole session, the 40 trials were performed in sequence, with a 10 seconds pause between each trial. For each target position to reach, a time limit was set so that if a highlighted target can not be reached within 2 seconds, the next target will automatically highlight.

D. Data Analysis

Given the sequence of wrist orientations R_i relative to each trial, the sequence of rotation vectors $\mathbf{r}_i$ were derived as follows:

$$\mathbf{r}_i = \frac{1}{1 + R_{i1,1} + R_{i2,2} + R_{i3,3}} \begin{bmatrix} R_{i3,2} - R_{i2,3} \\ R_{i1,3} - R_{i3,1} \\ R_{i2,1} - R_{i1,2} \end{bmatrix} \tag{2}$$

while the sequence of pointing vectors $\mathbf{n}_i$ can be found using eq. 1.

The second and the third components of the vector $\mathbf{n}_i$ are used to give a feedback to the subjects on the current position of the pointing vector on the screen (x and y screen coordinates). To assess motor learning during the visual perturbation and the aftereffects during the washout phase, we computed two indices, proposed by [11] to assess wrist movements in similar tasks:

- the A_{sum} index, which measures a paths total deviation from a straight line connecting start and end points of each movements (from the central target to a peripheral target or vice-versa);
- the A_{net} index, which indicates whether a path deviates more to one side than another and, if so, to which side.

Further details about the derivation of A_{sum} and A_{net} can be found in [11].

While the wrist pointing directions necessarily lie in a 2-dimensional space, the three components r_{xi}, r_{yi} and r_{zi} of a rotation vector $\mathbf{r}_i$, in general, define points of a 3-dimensional space. In Fig. 1-right, both the wrist pointing directions $\mathbf{n}_i$ (red circles) and the rotation vectors $\mathbf{r}_i$ (blue crosses) are represented. Our analysis confirmed previous results [6] in that the rotation vectors tend to lie on a 2-dimensional surface (Donders' law) which can be well approximated by a plane near the 'zero' position.

Numerically, as in [10], the sequence $\mathbf{r}_i = [r_{xi} \; r_{yi} \; r_{zi}]^T$ was fitted to $\mathbf{r^*}_i = [r^*_{xi} \; r_{yi} \; r_{zi}]^T$ where is r^*_{xi} is defined by a generic quadratic surface:

$$r^*_{xi} = C_1 + C_2 r_{yi} + C_3 r_{zi} + C_4 r^2_{yi} + 2C_5 r_{yi} r_{zi} + C_6 r^2_{zi} \tag{3}$$

where the coefficients $C_1 \ldots C_6$ were determined via nonlinear least-squares fitting methods. The first three coefficients (C_1, C_2 and C_3) define a plane, while the last three coefficients (C_4, C_5 and C_6) are related to the *curvature* of the fitted surface [6].

As in previous studies, the goodness of fit was expressed in terms of *thickness* of the best fitting surface (Donders' surface), and it is defined as the standard deviation of the fitting error between the sequence $\mathbf{r}_i$ and surface itself. Low values of thickness indicate that a soft constraint (such as

Donders law) apply to wrist kinematics during pointing tasks. Further details about data analysis for the estimation of Donders' surfaces can be found in [6].

III. Results

First of all, we quantify motor learning during adaptation, by analyzing the trajectories of the movements in the screen coordinates. Figure 2 shows the trajectory for one representative subject in the following trials: the last baseline trial, the first adaptation trial, the last adaptation trial, the first washout trial and the last washout trial. Data from each single movement were elaborated to calculate the A_{sum} and A_{net} in all trials. Figure 3 shows the average values of the two coefficients for the same representative subject. It can be noticed that trajectories are perturbed at the beginning of the adaptation phase, as indicated by a sudden increasing of the A_{sum} index; such index decreases with training during the following trails, while it increases again at the beginning of the washout phase and finally goes back to normal values at the end of the protocol. A_{net} exhibits similar behavior, with the difference that it takes also into account if a path deviates more to one side than another. Opposite signs of A_{net} index for inwards and outwards movements for the adaptation and washout phases demonstrate that CNS has learned a new internal model during adaptation, which produces aftereffects when the perturbation is removed, as demonstrated by previous studies [7]. Figure 4 A_{sum} and A_{net} shows that this behavior is consistent for all the tested subjects. Data demonstrated that subjects adapt their movements to the perturbation by creating a new internal model, also when the brain is committed in the execution of a redundant task.

Secondly, we tested whether motor strategies adopted to solve redundancy (i.e. Donders' law for the wrist) are held during the adaptation and washout processes, or if they are disrupted. Figure 5 shows thickness values of Donders' surfaces, averaged on all subjects, during the different phases of the protocol. Data show that thickness values, which indicate to what extent Donders' law applies to wrist movements, slightly increase during both adaptation and washout phases, if compared with baseline trials. Anyway, absolute values of thickness remain in the range of physiological values (1 to 3 degrees [6],[10]), demonstrating that Donders' law still applies during the adaptation and washout processes. Nevertheless, the increasing of thickness with respect to baseline values show that the adaptation to an external perturbation during a redundant task increase the "biological noise" associated to this kind of motor strategy [12],[13].

Finally, we evaluated if Donders' law, that has been shown to hold during the protocol, remains the same or if it itself adapts. Following the approach in [6], we analyzed the curvature of Donders' surfaces during the different phases of the protocol. In figure 6 Donders' surfaces of one representative subject are reported. It can be noticed that Donders' surfaces maintain similar characteristics during the whole protocol. This suggests that Donders' law for the wrist is not modified by motor adaptation. To statistically test this hypothesis, we

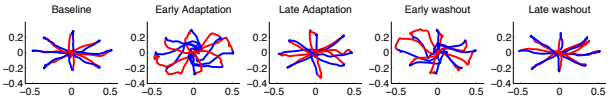

Fig. 2. Trajectories in screen coordinates for one representative subject in 5 trials of the experimental protocol. In red are represented movements from central to peripheral targets, while in blue the movements from peripheral to central target.

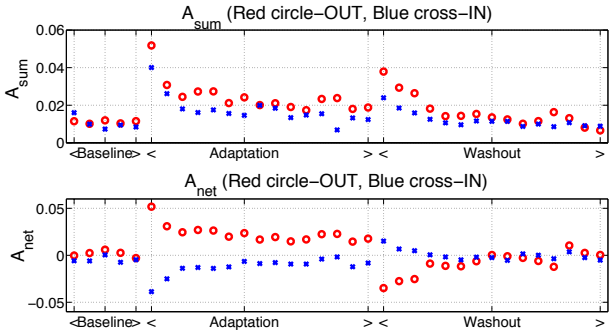

Fig. 3. A_{sum} and A_{net} indices in all trials for one representative subject. Red circles indicates movements from central to peripheral targets, while in blue crosses movements from peripheral to central target.

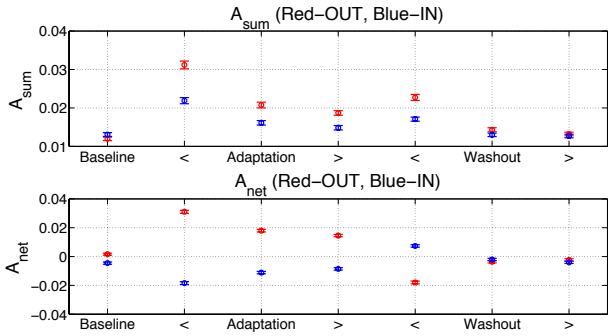

Fig. 4. Mean values $\pm$ Standard Error (SE) of A_{sum} and A_{net} indices averaged on all subjects in the different phases of the protocol (grouped in blocks of 5 trials). Red data indicates movements from central to peripheral targets, while blue ones movements from peripheral to central target.

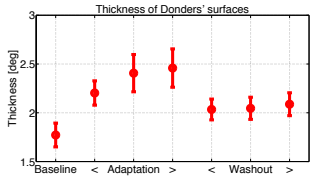

Fig. 5. Mean values $\pm$ Standard Error (SE) of the thickness of Donders' surfaces, averaged on all subjects in the different phases of the protocol (grouped in blocks of 5 trials).

performed a multivariate analysis of variance (MANOVA) on the multivariate vector of curvatures of Donders' surfaces This allows us to evaluate both within-subject and between-subjects variability during the different phases of the protocol. Such tests are summarized in Tab. I, where the main result of each test is determined by the value of D, which is an estimate of the dimension of the space containing the group means. MANOVA tests have been performed using the multivariate vector $[C_4, C_5, C_6]$ (see eq. 3) as dependent variable. In the Within-Subjects tests, the effect of the 3 protocol phases (baseline, adaptation and washout phases

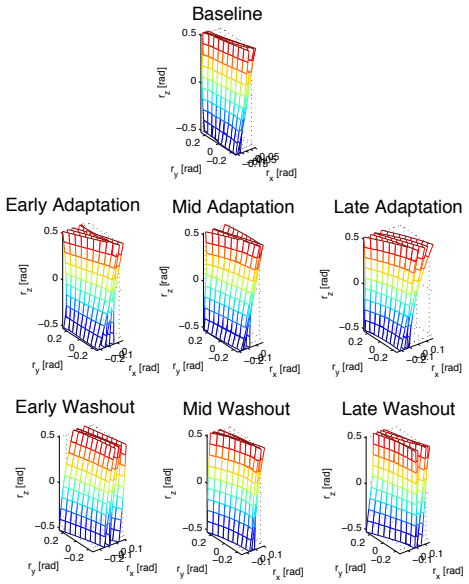

Fig. 6. Donders' surfaces for one representative subject in the different phases of the protocol (grouped in blocks of 5 trials).

have been used as independent variables) was analyzed. For the Between-Subjects tests, the 9 subjects were used as independent variables. The multivariate hypotheses are 'D=0', 'D=1' and for such hypotheses the relative p-values are reported in Tab. I . Results of the MANOVA tests show that for each subject curvatures of Donders' surfaces do not significantly change (D value is 1 for all subjects except subject 2) during the adaptation and washout processes, indicating that motor strategies, such as Donders' law, remain invariant during motor adaptation in redundant tasks. On the other hand, MANOVA analysis for testing between-subjects variability shows that Donders' surfaces curvature coefficients vary among subjects, confirming results in [6].

IV. CONCLUSIONS

In the present study we analyzed motor adaptation during a simple redundant tasks. Using an instrumented handle and a simple video-game, we measured wrist and forearm movements during pointing tasks and their adaptation to visual perturbation. The main objective of the this study is to investigate whether motor adaptation interferes on the strategies adapted by the brain to solve the redundancy. First, our analysis demonstrated that subjects adapt their movements to the perturbation, and exhibit classical aftereffects during the early stage of the washout phase, also when the brain is committed in the execution of a redundant task. Then, we showed that motor strategies used to solve redundancy (i.e Donders' law) are not disrupted during adaptation, since absolute values of thickness during the whole protocol remain in the range of physiological values (1 to 3 degrees [6],[10]). Nevertheless, we noticed an increasing of the "biological noise" associated to this kind of motor strategy during the adaptation and washout phases of the protocol, as thickness values exhibit a little increase in these two phases with respect to baseline values. Finally, we found that for each

Within Subjects	D	p-values for 'D=0' / 'D=1'
sbj 1	1	0.0001/0.4352
sbj 2	2	0.0000/0.0008
sbj 3	1	0.0007/0.8026
sbj 4	1	0.0002/ 0.0562
sbj 5	1	0.0001/ 0.2347
sbj 6	1	0.0000/ 0.5069
sbj 7	1	0.0305/ 0.0679
sbj 8	1	0.0000/ 0.4180
sbj 9	1	0.0046/ 0.8547
Between Subjects	3	0.0000/ 0.0000

TABLE I
SUMMARY TABLE FOR THE MANOVA TESTS.

subject curvatures of Donders' surfaces do not significantly change during the adaptation and washout phases, indicating that motor strategies, such as Donders' law, remain invariant during motor adaptation in redundant tasks.

V. ACKNOWLEDGMENTS

This work was partly founded by the European Union under the FP7-ICT program (IM-CLeVeR project, no. ICT-2007.3.2-231722), by the Italian Ministry of Education, University and Research under the FIRB - Futuro in Ricerca program (TOUM project, no. B81J10000160008), and by the Academic Research Fund (AcRF) Tier1 (RG 40/09), Ministry of Education, Singapore.

REFERENCES

[1] T. Flash and N. Hogan, The coordination of arm movements: an experimentally confirmed mathematical model, *The Journal of Neuroscience*, vol. 5, 1985, pp 1688-1703.
[2] Y. Uno, M. Kawato, R. Suzuki, Formation and control of optimal trajectory in human multijoint arm movement, *Biological Cybernetics*, vol. 61, 1989, pp 89-101.
[3] C. M. Harris and D.M. Wolpert DM, Signal-dependent noise determines motor planning, *Nature*, vol. 394, 1998, pp 780-784.
[4] J. P. Scholz and G. Schoner, The Uncontrolled Manifold Concept: Identifying Control Variable for a Functional Task, *Experimental Brain Research*, vol. 126, 1999, pp 289-306.
[5] E. Todorov and M. I. Jordan, Optimal feedback control as a theory of motor coordination, *Nature Neuroscience*, vol. 5, 2002, pp 1226-1235.
[6] D. Campolo, D. Formica, E. Guglielmelli, F. Keller, Kinematic analysis of the human wrist during pointing tasks, *Experimental Brain Research*, vol. 201, 2010, pp. 561-573.
[7] R. Shadmehr and F. A. Mussa-Ivaldi, Adaptive representation of dynamics during learning of a motor task, *The Journal of Neuroscience*, vol. 14, 1994, pp 3208-3224.
[8] O. Donchin, J. T. Francis, R. Shadmehr, Quantifying generalization from trial-by-trial behavior of adaptive systems that learn with basis functions: theory and experiments in human motor control, *The Journal of Neuroscience*, vol 23, 2003, pp 9032-9045.
[9] J. Diedrichsen, O. White, D. Newman, N. Lally, Use-Dependent and Error-Based Learning of Motor Behaviors, *The Journal of Neuroscience*, vol. 30, 2010, pp 5159-5166.
[10] D. Tweed and T. Vilis, Geometric Relations of Eye Position and Velocity Vectors during Saccades, *Vision Research*, vol. 30, 1990, pp 111-127.
[11] S. K. Charles and N. Hogan, The Curvature and Variability of Wrist and Arm Movements, *Experimental Brain Research*, vol. 203, 2010, pp 63-73.
[12] D. Campolo, D. Accoto, D. Formica, E. Guglielmelli, Intrinsic Constraints of Neural Origin: Assessment and Application to Rehabilitation Robotics, *IEEE Transactions on Robotics*, vol. 25, 2009, pp 492-501.
[13] N. L. Tagliamonte, M. Scorcia, D. Formica, D. Campolo, E. Guglielmelli, Effects of Impedance Reduction of a Robot for Wrist Rehabilitation on Human Motor Strategies in Healthy Subjects during Pointing Tasks, *Advanced Robotics*, vol. 25, 2011, pp 537-562.